Available online at www.sciencedirect.com

ScienceDirect

Procedia IUTAM 22 (2017) 39 – 50

Procedia IUTAM

www.elsevier.com/locate/procedia

IUTAM Symposium on Nonlinear and Delayed Dynamics of Mechatronic Systems

State dependent delayed drill-string vibration: Theory, experiments and new model

M. Wiercigroch[a,*], K. Nandakumar[a,b], L. Pei[a,c], M. Kapitaniak[a], V. Vaziri[a]

[a] *Centre for Applied Dynamics Research, School of Engineering, University of Aberdeen, Scotland, UK*
[b] *Lloyd's Register EMEA, Aberdeen, UK*
[c] *School of Mathematics and Statistics, Zhengzhou Univ., Zhengzhou, Henan 450001 China*

Abstract

We have reviewed the development and the analysis of the coupled two degrees-of-freedom model of drill-string vibration, which assumes a state-dependent time delay and a viscous damping for both the axial and torsional vibration. This model corrects the instability deficiencies of the previous models but it is still based on a uniform angular distribution of blades on a drill-bit, which can lead to unrealistic regenerative types of instability. However, the model sheds some lights on the origin and the interplay between stick-slip and bit-bounce, the dangerous dynamic phenomena encountered during rotary drilling. The experimental rig developed by the Centre of Applied Dynamics Research at the University of Aberdeen is used to show some shortcomings of this model and to develop a new more realistic one. The new model assuming a non-uniform distribution of blades for drag type drill-bits is proposed.

© 2017 The Authors. Published by Elsevier B.V. This is an open access article under the CC BY-NC-ND license (http://creativecommons.org/licenses/by-nc-nd/4.0/).

Peer-review under responsibility of organizing committee of the IUTAM Symposium on Nonlinear and Delayed Dynamics of Mechatronic Systems

Keywords: drill-string; vibration; state dependent delay; modelling; experiments

1. Introduction

Modelling of drill-string vibration is a challenging problem and has been the subject of intensive research for many years. The highly nonlinear nature of interactions between a drill-string and a borehole, where the formation couples the axial, torsional and lateral vibration, makes it difficult to study in a comprehensive manner. The literature on drill-string vibration is vast and a number of surveys have been written (e.g. [1,2]). Drill-strings primarily vibrate in axial, torsional and lateral modes, leading to bit-bounce, forward and backward whirling, and torsional vibration with its dangerous form of stick-slip.

Theoretically, drill-string vibration has been studied using lumped-mass models, Cosserat-continuum models and finite elements. However in this paper, we restrict our attention to the study of axial-torsional vibration by using a fully coupled two degrees-of-freedom model with a state-dependent time delay. And through the linear stability analysis

* Corresponding author. Tel.: +44-(0)1224-272509.
E-mail address: m.wiercigroch@abdn.ac.uk

2210-9838 © 2017 The Authors. Published by Elsevier B.V. This is an open access article under the CC BY-NC-ND license (http://creativecommons.org/licenses/by-nc-nd/4.0/).
Peer-review under responsibility of organizing committee of the IUTAM Symposium on Nonlinear and Delayed Dynamics of Mechatronic Systems
doi:10.1016/j.piutam.2017.08.007

the stable and unstable operating regimes will be discussed in the control parameter space comprised of Weight On Bit (WOB) and rotary speed. This model assumes a uniform angular distribution of blades which leads to regenerative effects type of instabilities, which will be challenged via our experimental studies.

Many experimental rigs to investigate drill-string vibration have been reported in the literature, where their designs and capabilities vary according to their purposes. These rigs can be classified in two groups. The first group contains large-scale test beds. Such systems are similar to real drilling rigs used in the field. Early experimental investigations of PDC drill-bits for their whirling tendencies, were discussed in [3]. The authors of [4] reported on a large-scale laboratory rig capable of drilling with a range of drill-bit diameters under WOB, rotary speed and hydraulic conditions similar to that experienced in field. In [5] torsional vibration experiments in a nearly vertical, 1000 meter deep, full scale research drilling rig were presented. These types of the drilling test rigs are expensive to use and difficult to access.

The second group includes scaled laboratory stands, which are designed to investigate particular phenomena under limited space in the laboratory. Some of these rigs were reviewed in [6]. Most of these rigs consist of a slender steel drill-string driven at the top by an electric motor. The drill-bit and Bottom Hole Assembly (BHA) are usually represented as cylinders. The presence of rock and the cutting action is usually simulated through shakers and brakes. Standard axial excitations and torque profiles are applied onto through these shakers and brakes. Typical examples of this type of experimental apparatus can be found in [7,8,9]. The authors of [10] presented a new scaled rig consisting of a rotating shaft representing a section of the BHA between two stabilizers for reproducing lateral drill-string vibration with and without contact. In contrast to these cases, the rig in [11] is designed to drill actual rocks. In that setup the rock is given rotary motion, while the drill-bit and BHA are stationary. The torsional flexibility of the drill-pipes is simulated through a special gear-pulley-spring system. This rig, although drilling in real rocks, neglects the lateral dynamics of the BHA.

The structure of this paper is as follows. In Section 2, the state-of-the-art in modelling and analysis of the drill-string vibration will be introduced. Recently, there has been a significant interest in modelling of regenerative effects and their influence on torsional and axial vibration [12,13,14,15,16]. All these investigations have been only theoretical and the main hypothesis is a potential similarity with the regenerative effect in metal cutting, which has a strong experimental evidence. Section 3 discusses briefly a new experimental rig developed by the Centre for Applied Dynamics Research at the University of Aberdeen. This rig is one of the most comprehensive experimental setups worldwide, allowing to study all important effects occurring in drill-string vibration and also the drill-bit and rock interactions. In Section 4, a new drill-string dynamics model is postulated, where the main assumption of uneven spacing between blades of a drag bit is relaxed. The uneven distribution of blades (cutters) is the norm for all commercial drill-bits and from the point of view of mathematical modelling would have significant consequences. The closing remarks are drawn in Section 5.

2. A two degrees-of-freedom axial-torsional model

In this section, we present the derivation and analysis of a coupled two degrees-of-freedom model for axial and torsional vibration of a drill-string with uniform distribution of blades. The material presented in this section is a summary of the work presented in [17,18]. The reader is referred to [17] for more details.

The starting point for the model developed in [17] is the work of [19], where the derivation of cutting and friction forces remains unchanged. However, the model of [19] did not consider axial stiffness and dissipation of energy in drill-pipes. This situation has been partially remedied in another work [20] by addition of an axial dissipation and compliance. In our work [17], the model presented in [17,19] was further enhanced by incorporating a torsional dissipation. For the so-derived fully coupled model, a detailed linear stability analysis was performed. Through the linear stability analysis the stable and unstable operating regions caused by a regenerative effect in the WOB-rotary speed parameter plane will be revealed.

Figure 1 shows the physical model as a two degrees-of-freedom system (one axial, and one torsional) to model the axial and torsional vibrations of drill-strings. The torsional part of the model idealizes a drill-string as a torsional pendulum. The combined rotational inertia of the BHA and drill-pipes is denoted by I, while the drill-pipe's torsional stiffness is modeled by a linear torsional spring of stiffness K. The top end of the torsional spring is assumed to rotate with a constant spin speed Ω_0. The rotation of the bottom end is monitored by the angle Φ from a fixed reference. The Torque-On-Bit (TOB) T arising from the bit-rock interactions is applied to the rotational inertia.

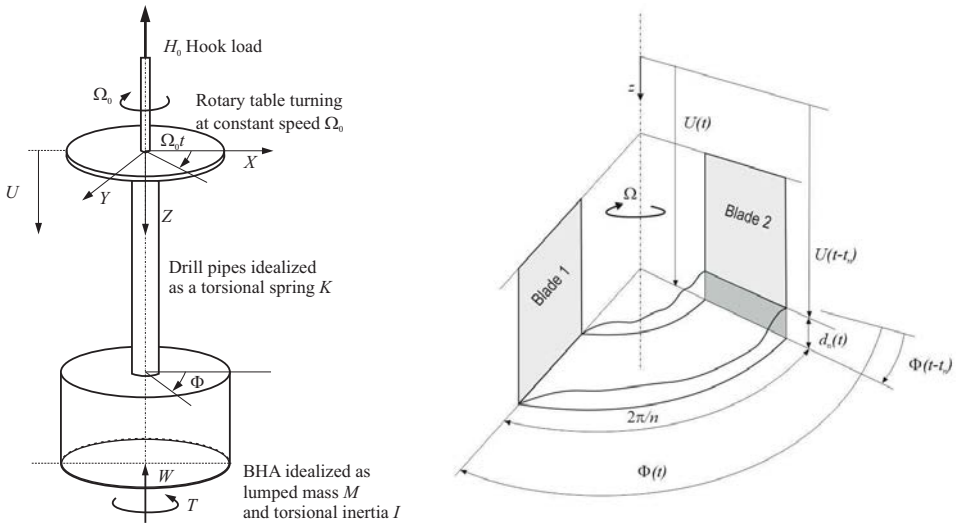

Fig. 1. Left: Physical model of the axial-torsional vibration as presented in [19]. The model has two degrees-of-freedom (translation U, and rotation Φ of the bit). The rotary table at the top is driven at constant angular velocity Ω_0 and a hook load H_0 is applied to top of drill-pipes. Reactions from rock, W, and the reactive torque, T, are acting on the BHA. Right: Schematic of a drag bit illustrating the definition of the instantaneous depth of cut. Two successive blades of the bit are shown. The instantaneous depth of cut faced by a blade (say 2) equals the difference between the present axial position of the bit and its position at an earlier instant when the immediately preceding blade (say 1) was occupying the current angular position of blade 2. Adopted from [17].

The axial part of the model idealizes a BHA and a drill-string as a lumped mass M by neglecting the axial compliance of drill-pipes. A constant vertical hook load H_0 (which is related to the applied WOB) is applied at the top of the mass M and the force W arising from the bit-rock interactions is applied on the mass as shown in Fig. 1. The axial displacement of the drill-bit is measured by U from a fixed reference.

2.1. Cutting and friction forces

The axial force and torque exerted by the rock on the bit is decomposed into the cutting and friction components denoted by appropriate subscripts. The cutting and friction components of the force and torque are derived based on cutting experiments using single cutters on a variety of rocks as reported in [21,22]. Thus we have

$$T = T_c + T_f\,, \quad W = W_c + W_f\,, \tag{1}$$

where

$$T_c = \frac{a^2\,\epsilon\,d}{2}\,, \quad W_c = \xi\,\epsilon\,a\,d\,. \tag{2}$$

Here a represents the radius of the bit, d represents the instantaneous depth of cut, ϵ represents the intrinsic specific energy of the rock (see [21,22] for details) and ξ characterizes the inclination of the cutting forces on the cutting face.

The friction components of the TOB and WOB are given by

$$W_f = \sigma\,a\,l\,, \quad T_f = \frac{\mu\,\gamma\,a\,W_f}{2}\,, \tag{3}$$

where the parameter γ is related to the orientation of the cutters on the bit, σ refers to the maximum contact pressure at the bit-rock interface, and l refers to the total wear-flat length in all the blades.

To define the instantaneous depth of cut d, we consider an idealized drag bit with n blades, where the kinematics of two consecutive blades are shown in the right panel of Fig. 1. The instantaneous depth of cut by each blade is the

difference between the present axial position of the bit and the axial position occupied by the bit $1/n$-th revolution ago.

Thus the instantaneous depth of cut faced by a single blade (say 2, shown in the right panel of Fig. 1) is given by

$$d_n = U(t) - U(t - t_n), \tag{4}$$

where t_n is the time taken by the bit to rotate by an angle equal to $\frac{2\pi}{n}$. Thus the time delay $t_n(t)$ satisfies the following equation

$$\Phi(t) - \Phi(t - t_n) = \frac{2\pi}{n}\,. \tag{5}$$

As all instantaneous depths of cut are the , the total depth of cut per revolution for n blades is

$$d = n\,(U(t) - U(t - t_n))\,.$$

In the absence of torsional oscillations, the drill-bit would rotate with a constant angular velocity Ω_0 and the time delay $t_n = \frac{2\pi}{n\,\Omega_0}$ would be a constant. However, when the drill-string undergoes torsional vibration, the time delay itself is governed by the system dynamics through Eq. (5). It is worth emphasizing here that the state-dependent nature of the time delay makes the analysis complicated.

2.2. Improved physical model[17]

In addition to the contact and cutting forces derived earlier, the viscous dissipation and system stiffness are incorporated now in order to derive the final equations of motion. A schematic of the improved physical model is presented in Fig. 2.

The torsional part of the model is similar to that of Fig. 1 with the addition of torsional viscous damping C_t. The top end of the torsional spring representing the rotary table, is turned with a constant angular velocity Ω_0. Thus the angular position of the top end is $\Phi_0 = \Omega_0\,t$, as shown in Fig. 2.

In the axial part of the model the inertia of the BHA and the drill-pipes is lumped together as the mass M, while the elasticity of the drill-pipes is idealized as a spring of stiffness K_a. The top end is assumed to move axially with a constant velocity V_0, which corresponds to the steady state penetration rate. Thus the axial position of the top end is $U_0 = V_0\,t$.

2.3. Equations of motion and stability[17]

With the idealisation introduced in previous subsections, the final equations of motion of the axial and torsional motions are

$$M\,\ddot{U} + C_a\,\dot{U} + K_a(U - V_0\,t) = W_0 - \xi\,a\,\epsilon\,d\;H(\dot{\Phi})\;H(d) - W_f\,H(\dot{U})\,, \tag{6}$$

$$I\,\ddot{\Phi} + C_t\,\dot{\Phi} + K_t\,(\Phi - \Omega_0\,t) = -\frac{a^2\,\epsilon\,d}{2}\,H(d)\,H(\dot{\Phi}) - \frac{\mu\,\gamma\,a\,W_f}{2}\,\mathrm{sgn}(\dot{\Phi})\,H(\dot{U})\,, \tag{7}$$

where

$$d = n\,(U(t) - U(t - t_n))\,, \tag{8}$$

and

$$\Phi(t) - \Phi(t - t_n) = \frac{2\pi}{n}\,. \tag{9}$$

In Eqs 6 and 7, d_0 represents the steady-state of depth of cut and W_0 is the force required for steady drilling, which is physically provided by the self-weight of the system. Equations (6) - (9) constitute a set of two coupled delay differential equations with a state-dependent delay implicitly defined through Eq. (9) along with the discontinuities associated with the cutting and friction forces. The dynamics of the full nonlinear system is complex and analytical

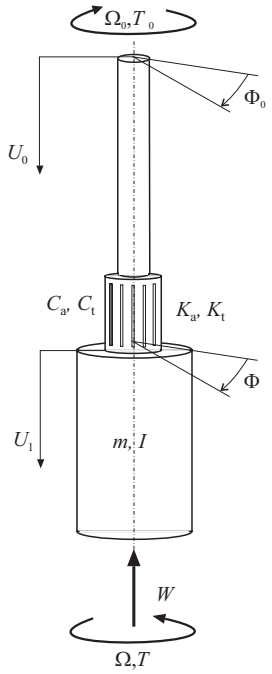

Fig. 2. Schematic of the drill-string model with a lumped mass approximating the BHA (m, I), and a flexible cylinder modeling the stiffness (K_a, K_t) and damping (C_a, C_t). The model shows a constant rate of descent imposed at the top, in addition to all other elements of Fig. 1. Adopted from [17].

treatment is difficult. However, the steady state drilling with a constant Rate Of Penetration (ROP) and its stability are important from the engineering point of view.

Steady drilling corresponds to a constant rate of penetration V_0 while rotating at a constant angular velocity Ω_0. By introducing axial, torsional and delay perturbations to the steady system, and then by applying appropriate non-dimensional variables and parameters, the linearized equations of motion used for stability analysis are [17]

$$x'' + 2\zeta\beta x' + \beta^2 x = n\psi\left[\frac{v_0}{\omega_0}(\phi - \phi(\tau - \hat{\tau}))\right] - n\psi(x - x(\tau - \hat{\tau}))\,, \tag{10}$$

$$\phi'' + 2\kappa\phi' + \phi = n\left[\frac{v_0}{\omega_0}(\phi - \phi(\tau - \hat{\tau}))\right] - n\,(x - x(\tau - \hat{\tau}))\,. \tag{11}$$

By introducing the exponential solutions in Eqs 10-11 and defining $v = \dfrac{v_0}{\omega_0}$, the characteristic equations of the system are

$$(\lambda^2 + 2\zeta\beta\lambda + \beta^2)(\lambda^2 + 2\kappa\lambda + 1) - nv\left(1 - e^{-\frac{2\pi\lambda}{n\omega_0}}\right)(\lambda^2 + 2\zeta\beta\lambda + \beta^2) + n\psi\left(1 - e^{-\frac{2\pi\lambda}{n\omega_0}}\right)(\lambda^2 + 2\kappa\lambda + 1) = 0\,.$$

The stability boundaries are obtained by substituting $\lambda = i\omega$ into the characteristic equations. After consideration of various stability lobes (see [17]), the final stability curves demarcating the stable and unstable operating parameters obtained for representative values of a typical drill-string and BHA assembly are presented in Table 1 and plotted in Fig. 3.

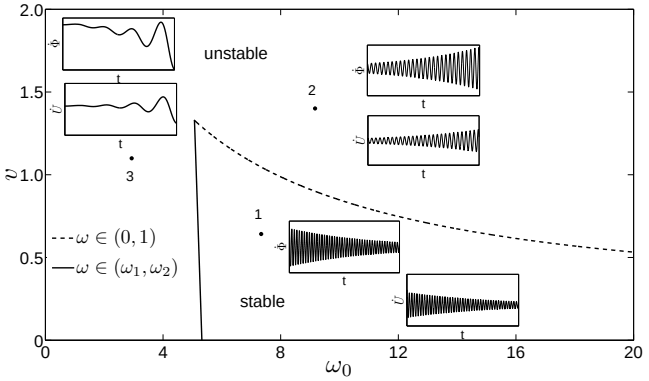

Fig. 3. Stability boundaries computed from Eqs (10)- (11) for the parameters given in Table 1 of [17]. The stable and unstable regions herein were determined by considering the crossing of eigenvalues across the curves for all ks. Three parameter sets labeled 1 through 3 in the plot have been chosen in the stable and unstable regimes. The three parameter pairs are respectively: 1) $\omega_0 = 7.336, v = 0.6417$. 2) $\omega_0 = 9.170, v = 1.401$. 3) $\omega_0 = 2.934, v = 1.099$. Three pairs of time histories (each pair consisting plots of $\dot{U}$ and $\dot{\Phi}$) corresponding to the three parameter points, generated through numerical simulations of Eqs (6)-(9), are plotted along side the parameter labels. These time histories reveal the stability nature of the corresponding parameters. See [17] for further details regarding the simulations. Adopted from [17].

Table 1. List of the parameter values utilized for generation of stability charts (values adopted from [22]).

Parameter	Symbol	Value	Unit
Drill-pipe axial stiffness	K_a	$7.0 \cdot 10^5$	N/m
Drill-pipe mass	M_{dp}	$2.8 \cdot 10^4$	kg
Drill-pipe torsional stiffness	K_t	940	N m/rad
Drill-pipe mass moment of inertia	I_{dp}	97	kg m^2
BHA mass	M_{bha}	$2.5 \cdot 10^4$	kg
BHA mass moment of inertia	I_{bha}	83	kg m^2
Vibrational mass	M	$3.4 \cdot 10^4$	kg
Vibrational mass moment of inertia	I	115.3	kg m^2
Radius of bit	a	0.108	m
Wear flat length	l	0.0012	m
Rock specific strength	ϵ	60	MPa
Contact pressure	σ	60	MPa
Coefficient of friction	μ	0.6	-
Cutter inclination coefficient	ξ	0.6	-
Axial damping coefficient	ζ	0.01	-
Torsional damping coefficient	κ	0.01	-
Axial-to-torsional frequency ratio	β	1.58	-
Number of blades	n	4	-
Cutter inclination parameter	ψ	13.90	-

3. Aberdeen Drill-string Dynamics Experimental Rig

3.1. Experimental rig main components

The Aberdeen Drill-string Dynamics Experimental Rig [23] described below, is one of the most comprehensive experimental setups worldwide, that allows to study all the important phenomena in drill-string dynamics, including

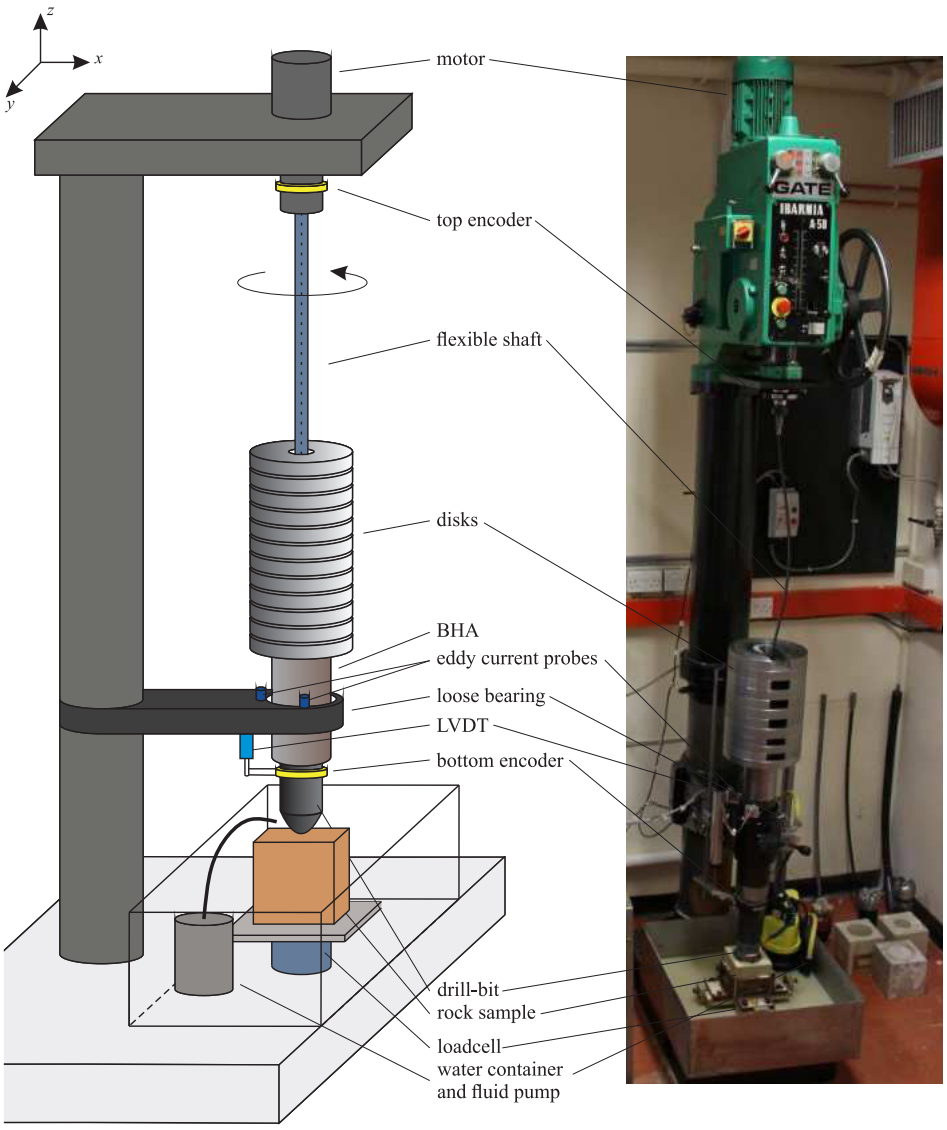

Fig. 4. Schematic (left) and photograph (right) of the Aberdeen Drill-string Dynamics Experimental Rig showing its main components such as BHA, flexible shaft, WOB disks, drill-bit, rock sample and motor. the instrumentation include load-cell, LVDT, top and bottom encoders and eddy current probes. Adopted from [23].

stick-slip, whirling and bit bounce as well as the interactions between the drill-bit and the rock. The main components of this experimental setup depicted in Fig. 4, can be grouped in three categories:

- drill-string composed of flexible/rigid shaft, BHA, WOB disks, and the drill-bit,
- rock samples and cutting fluid circulation system and
- sensors, instrumentation and Data Acquisition System (DAQ).

The rig has been designed to operate either with a rigid or a flexible shaft. The configuration with the rigid shaft allows to determine mechanical characteristics of drill-bits, specifically relationships between ROP and WOB, ROP and rotary speed and others. The configuration with the flexible shaft is used to simulate all dynamic phenomena occurring during downhole drilling including stick-slip, whirling and bit bounce. The drill-string is driven by an

electric motor, which angular velocity ranges from 0.5 to 1370 rpm. A drill-pipe connects the motor with the BHA, which transmits the rotary motion to the drill-bit by means of a bit-holder attached at the bottom end of the BHA. At the other end, the flexible shaft is connected to the BHA made as a heavy steel shaft, which is restrained to move in transversal direction by a loose bearing. The drilling machine is equipped with the spindle allowing axial movement of the top of the drill-string in the range 0 to 220 mm. An axial static force or a WOB is realized in this experimental setup by placing steel disks on the top of the BHA. In this it is possible to provide WOB within the range 0.93 kN to 2.79 kN. At the end of the BHA, commercial drill-bits are attached (both PDC and RC can be used) and placed on the top of rock sample. In our studies we have used various rocks including sandstone, granite, limestone. A rock sample is fixed at the bottom of the rig by a rock holder. In the system, water is used as drilling fluid, which removes debris and heat. The debris are driven by gravity to the bottom of the tank.

A variety of different sensors are used in the experimental setup, which allow us to conduct detailed measurements of the most important parameters of the drilling process. These include two rotary encoders to measure top and bottom angular velocity, two eddy current probes to measure displacement of the BHA inside the borehole and an axial position transducer to monitor Rate of Penetration (ROP). The most advanced sensor in our setup is the four component dynamometer (Kistler 9272) placed directly below the rock sample, which allows to measure static and dynamic forces including, axial force, torque and two forces acting in transversal directions x and y as depicted in Fig. 4. The measured torque and forces are within the ranges of 0-200 Nm and 0-20 kN respectively.

3.2. Experimental studies

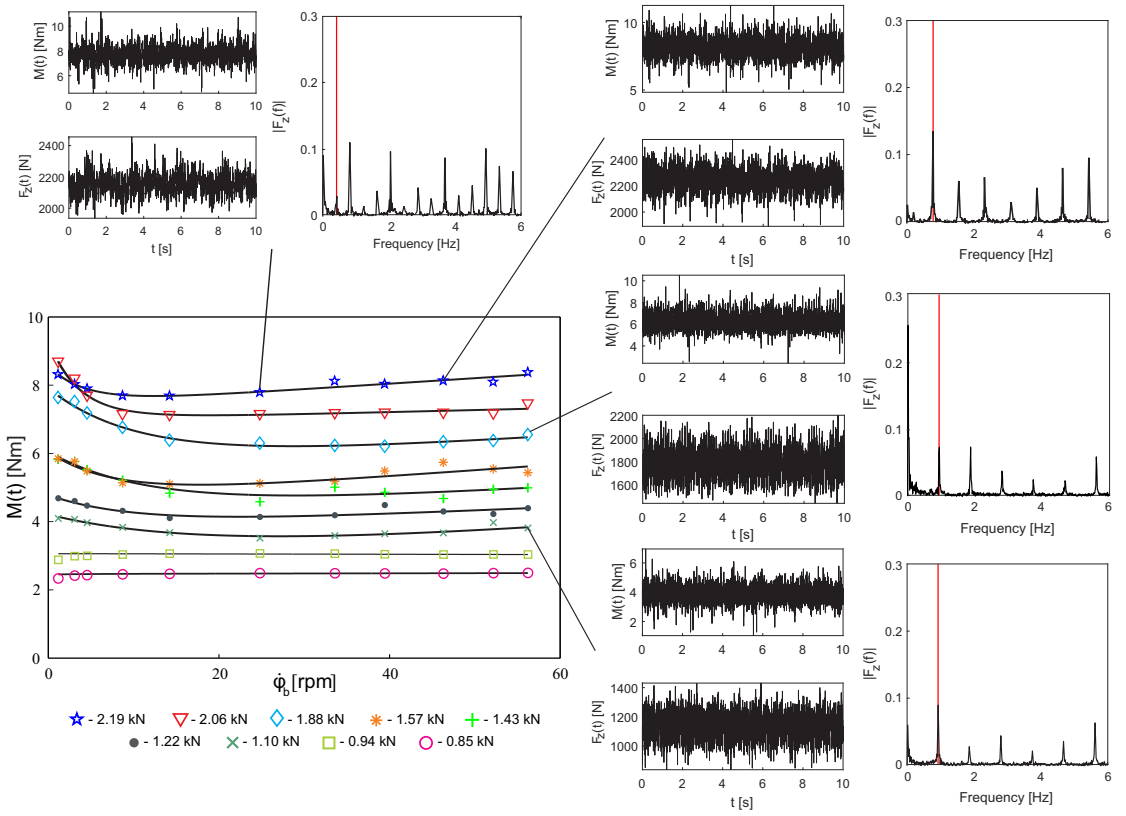

Fig. 5. Experimental studies of the interactions between a drill-bit a drilled formation. The main panel shows the results of the identification of TOB curves for different values of WOB. The other 4 sets of panels show times histories of $F_z(t)$ and $M(t)$ recorded when constructing the the mechanical characteristics for the investigated drill-bit, TOB vs $\dot{\varphi}_b$. The red spikes on the power spectra are the frequencies of the drill-bit rotation.

In order to get more insight into the bit-rock interactions, dedicated experiments to establish relationship between Torque On Bit (TOB) and angular velocity of bit, were carried out. For this purpose, the flexible shaft is replaced by the rigid one and equivalent TOB while drilling is measured. The torque was measured for 9 different values of WOB between 0.85 and 2.19 kN), and for 11 rotational speeds ranging from 0.5 to 54 rpm. The procedure for determining the TOB characteristic was as follows. For a given number of steel disks providing a constant WOB, the rotational speed was varied in steps, for which the average steady state TOB was recorded. The steps were not fixed but chosen in such a way to obtain more readings for low angular speeds in order to ensure a higher accuracy of the TOB estimation near zero angular velocity. The TOB curves as a function of angular speed for different values of WOB, are shown in Fig. 5. It can be seen that the higher the WOB is, the higher TOB is observed. Moreover, a well known frictional phenomenon of decreasing torque values with increasing rotational speed is also visible. However, after reaching a certain threshold, the TOB starts to increase with an increased rotational speed. As shown in the main panel of Fig. 5, this behaviour is visible in a wide range of the analyzed WOB values. Interestingly, for WOB below 1.10 kN, this phenomenon was no longer observed. Instead, the TOB has a constant value along the considered range of rotational speeds. The time histories of dynamic values of WOB and TOB together with the power spectrum from the dynamic WOB shown on four sets of panels were depicted to discuss the nature of these dynamic forces. Looking at these time histories and the spectra, it is clear that there is no apparent regenerative effect. The results presented here were obtained with the drill-bit shown in the left panel of Fig. 6. As this drill-bit has 5 blades, a large spike at frequency around 5 times larger than the frequency of the drill-bit rotation (marked in red) should be visible, if the regenerative was dominating the dynamics of the drilling process. Such a behaviour has been observed over few years during our experimental studies [24,25], where we have thoroughly investigated the dynamics of BHAs and drill-strings.

Fig. 6. Examples of rock samples showing the patterns caused by the dynamic interactions with a drill-bit. The left panel shown one of the drill-bits used in our studies having 5 blades with their uneven distribution. As can be seen there is no vertical periodic patterns on the circles forming bottom hole.

4. New Model with Non-uniform Distribution of Blades

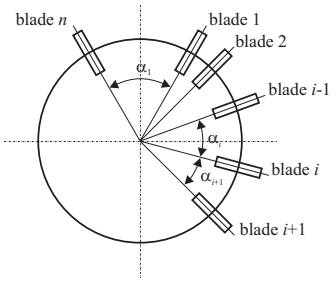

Fig. 7. Schematic of nonuniform angular blades distribution for a drag drill-bit. The angle α_i is constant as the drill-bit is considered as as rigid body.

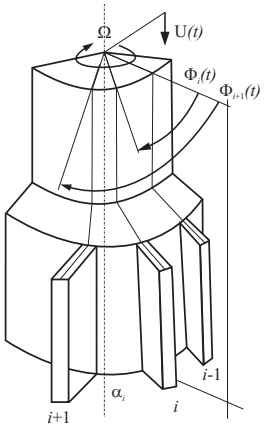

Fig. 8. Schematic showing angular and axial kinematics of a drill-bit with nonuniform blades distribution. This is a significant simplification as in a real drill-bit the so-called blade is a made of individual cutters, whose locations can differ from a single plane as has been postulated here.

Let us consider a drag drill-bit having n blades with not uniform angular distribution as shown in Fig. 7. The sum of all angles is equal to 2 π,

$$\sum_{i=1}^{n} \alpha_i = 2\pi. \tag{12}$$

The drill-bit rotates with the angular velocity Ω. Hence at the time t, its angular and axial displacements are $\Phi(t)$ and $U(t)$ respectively, which is schematically depicted in Fig. 8. An angular relationship between two neighbouring blades can be written as,

$$\Phi_{i+1}(t) - \Phi_i(t) = \alpha_{i+1}, i = 1, 2, ..., n \quad and \quad \Phi_{n+1}(t) = \Phi_1(t), \quad \alpha_{n+1} = \alpha_1. \tag{13}$$

Let assume that the total depth of cut per revolution to be '$d(t)$', which is the sum of the depth of cut from each individual blade

$$d(t) = \sum_{i=1}^{n} d_i(t). \tag{14}$$

For each blade, the depth of cut is different and can be described as

$$d_i(t) = U(t) - U(t - \tau_i). \tag{15}$$

Hence

$$d(t) = nU(t) - \sum_{i=1}^{n} U(t - \tau_i). \tag{16}$$

It is important to stress out here that a time delay τ_i is a function of time t,

$$\tau_i = \tau_i(t), \tag{17}$$

but for the sake of clarity, we will simply write it as τ_i.

Let us denote the total delay $\tau(t)$, i.e., the time taken by a bit to complete a full revolution. Thus the total depth $d(t)$ of cut per revolution is

$$d(t) = U(t) - U(t - \tau(t)), \tag{18}$$

which occurs when the bit made a full revolution

$$\Phi(t) - \Phi(t - \tau(t)) = 2\pi. \tag{19}$$

The contributing depths of cut, $d_1(t), ..., d_i(t), ..., d_n(t)$ can be calculated as the difference between the current position of the drill-bit $U(t)$ and their positions, $U_1(t), ..., U_i(t), ..., U_n(t)$. The time delays $\tau_1(t), ..., \tau_i(t), ..., \tau_n(t)$ are used to compute the contributing depth of cut as follows

$$\begin{aligned} d_1(t) &= U(t) - U_1(t) = U(t) - U(t - \tau_1(t)), \\ d_2(t) &= U(t) - U_2(t) = U(t) - U(t - \tau_2(t)), \\ &\vdots \\ d_i(t) &= U(t) - U_i(t) = U(t) - U(t - \tau_i(t)), \\ &\vdots \\ d_n(t) &= U(t) - U_n(t) = U(t) - U(t - \tau_n(t)). \end{aligned} \tag{20}$$

All contributing delays $\tau_i(t), i = 1, 2, ..., n$ and the total delay $\tau(t)$ are state-dependent. In the absence of torsional oscillations, the drill-bit would rotate at a constant angular velocity Ω, and then the time delay τ_i would be a constant. But when the drill-string undergoes torsional oscillations, the time delay itself is governed by the system dynamics, which is being currently investigated by the authors. The state-dependent nature of the time delay makes the analysis complicated.

If there is only one blade in the drag bit, then the blade force $F(t)$ will be proportional to the instantaneous depth of cut $d(t)$. Similarly, if there are n blades in the drag bit and their depthes $d(t)$ of cut are same, then the blades force $F(t)$ will be proportional to the depth of cut $nd(t)$. In case of a tool with non-uniformly distributed blades, the total force $F(t)$ will be a sum of contributing forces from each blade force $F_i(t), i = 1, 2, ..., n$, i.e.,

$$F(t) = \sum_{i=1}^{n} F_i(t), \tag{21}$$

where the contributing force $F_i(t)$ is also dependent on the instantaneous depth of cut $d_i(t)$.

After the substituion of (16) into the original EOMs given in[17], the EOMs for a drag drill-bit with non-uniform angular blade distribution is given as

$$\begin{aligned} M\ddot{U}(t) &= W_0 - \xi a\epsilon(nU(t) - \sum_{i=1}^{n} U(t - \tau_i(t)))H(\dot{\Phi}) - w_f H(\dot{U}), \\ I\ddot{\Phi}(t) + K(\Phi - \Omega_0 t) &= -\frac{a^2\epsilon}{2}(nU(t) - \sum_{i=1}^{n} U(t - \tau_i(t)))H(\dot{\Phi}) - \frac{\mu\gamma a w_f}{2} sgn(\dot{\Phi})H(\dot{U}). \end{aligned} \tag{22}$$

All the parameters $W_0, \xi, a, \epsilon, \sigma, l, K, \mu, \gamma$ and the functions $H(.)$ and $sgn(.)$ are same to those in[17]. The obtained EOMs, Equ. (22), will be use to model and analyse the dynamics of the downhole drilling process with drag drill-bits, which do not exhibit regenerative effects.

5. Closing Remarks

In this paper we have critically reviewed the development and the analysis of the coupled two degrees-of-freedom models to capture the dynamics of drill-strings. We have discussed our earlier model, which assumes a state-dependent time delay and a viscous damping for both the axial and torsional vibration. This model corrects the previous models, which were inherently unstable. Our model[17] sheds some lights on the origin of the observed complex phenomena and the interplay between stick-slip and bit-bounce, dangerous dynamic behaviour encountered during rotary drilling. All the current models assume a uniform angular distribution of blades on a drag drill-bit, which in consequence leads to regenerative types of instabilities. It is important to emphasize here, that there is no convincing experimental evidence of such instabilities.

Thus, we have undertaken studies on the Aberdeen Drill-string Dynamics Experimental Rig and by examining the experimental data, we have argued that real drag drill-bits are not responsible for regenerative effects. On contrary,

real drill-bits are designed not to introduce periodically varying forces. We have postulated that the main reason for this hypothesis is a non-uniform angular distribution of blades and based on this assumption we have formulated a new mathematical model, which does not poses the shortcomings of the previous ones. Specifically, the state-dependent nature of the time delay leading to the periodic excitation related to the rotational speed and the number of blades have been significantly modified. The dynamics yielding from his new modelled will be carefully studied in our future work.

Acknowledgements

L.J. Pei would like to acknowledge NNSF of China (No. 11372282) and China Scholarship Council.

References

1. P. D. Spanos, A. M. Chevallier, N. P. Politis, M. L. Payne, Oil well drilling: A vibrations perspective, The Shock and Vibration Digest 35(2) (2003) 81–99.
2. K. A. MacDonald, Failure analysis of drillstrings and bottom hole assembly components, Engineering Failure Analysis 1(2) (1994) 91–117.
3. J. M. Hanson, Dynamics modeling of PDC bits, in: SPE/IADC29401, SPE/IADC Drilling Conference and Exhibition, Amsterdam, The Netherlands, 26 February - 2 March 1995.
4. T. M. Warren, Drilling model for soft-formation bits, in: SPE8438, 54th SPE Annual Technical Conference and Exhibition, Las Vegas, 23 -26 September 1979.
5. G. W. Halsey, A. Kyllingstad, T. V. Aarrestad, D. Lysne, Drillstring torsional vibrations: Comparison between theory and experiment on a full-scale research drilling rig, in: SPE15564, 61st SPE Annual Technical Conference and Exhibition, New Orleans, Louisiana, 5-8 October 1986.
6. P. A. Patil, C. Teodoriu, A comparative review of modelling and controlling torsional vibrations and experimentation using laboratory setups, Journal of Petroleum Science and Engineering 112 (2013) 227–238.
7. Y. A. Khuleif, F. A. Al-Sulaiman, Laboratory investigation of drill-string vibration, Proceedings of the IMech E Part C: Journal of Mechanical Engineering Science 223 (2009) 2249–2262.
8. N. Mihajlović, A. A. van Veggel, N. van de Wouw, N. H., Analysis of friction-induced limit cycling in an experimental drill-string system, ASME Journal of Dynamic Systems, Measurement, and Control 124 (2004) 709–720.
9. C. Liao, B. Balachandran, M. Karkoub, Y. Abdel-Magid, Drill-string dynamics: Reduced-order models and experimental studies, Journal of Vibration and Acoustics 133 (4) (2011) 041008–1–041008–8.
10. H. Westermann, I. Gorelik, J. Rudat, V. AG, C. Moritz, M. Neubauer, J. W. O. Hohn, A new test rig for experimental studies of drillstring vibrations, SPE Drilling & Completion 30 (2) (2015) 119–128.
11. O. J. M. Hoffmann, Drilling induced vibration apparatus, Ph.D. thesis, University of Minnesota (2006).
12. A. Depouhon, E. Detournay, Instability regimes and self-excited vibrations in deep drilling systems, Journal of Sound and Vibration 333 (7) (2014) 2019–2039.
13. N. A. H. Kremers, E. Detournay, N. van de Wouw, Model-based robust control of directional drilling systems, IEEE Transactions on Control Systems Technology 24 (1) (2016) 226–239.
14. X. Liu, N. Vlajic, X. Long, G. Meng, B. Balachandran, Multiple regenerative effects in cutting process and nonlinear oscillations, International Journal of Dynamics and Control 2 (1) (2014) 86–101.
15. X. Liu, N. Vlajic, X. Long, G. Meng, B. Balachandran, State-dependent delay influenced drill-string oscillations and stability analysis, Journal of Vibration and Acoustics 136 (5) (2014) 051008–1–051008–9.
16. X. Liu, N. Vlajic, X. Long, G. Meng, B. Balachandran, Coupled axial-torsional dynamics in rotary drilling with state-dependent delay: stability and control, Nonlinear Dynamics 78 (3) (2014) 1891–1906.
17. K. Nandakumar, M. Wiercigroch, Stability analysis of a state dependent delayed model for drill-string vibrations, Journal of Sound and Vibration 332(10) (2013) 2575–2592.
18. K. Nandakumar, M. Wiercigroch, Galerkin projections for state-dependent delay differential equations with applications to drilling, Applied Mathematical Modeling 37 (2013) 1705–1722.
19. T. Richard, C. Germay, E. Detournay, A simplified model to explore the root cause of stick-slip vibrations in drilling systems with drag bits, Journal of Sound and Vibration 305 (2007) 432–456.
20. B. Besselink, N. van de Wouw, H. Nijmeijer, A semi-analytical study of stick-slip oscillations in drilling systems, Journal of Computational and Nonlinear Dynamics 6 (2010) 021006–1–021006–8.
21. E. Detournay, P. Defourny, A phenomenological model for the drilling action of drag bits, International Journal of Rock Mechanics and Mining Sciences 29 (1) (1992) 13–23.
22. E. Detournay, T. Richard, M. Shepherd, Drilling response of drag-bits: Theory and experiments, International Journal Rock Mechanics and Mining Science (2008) 1347–1360.
23. M. Kapitaniak, V. Vaziri Hamaneh, J. Páez Chávez, K. Nandakumar, M. Wiercigroch, Unveiling complexity of drillstring vibrations: Experiments and modelling, International Journal of Mechanical Sciences 101-102 (2015) 324–337.
24. M. Kapitaniak, Nonlinear Dynamics of Drill-Strings, Ph.D. thesis, University of Aberdeen (2015).
25. V. Vaziri, Dynamics and Control of Nonlinear Engineering Systems, Ph.D. thesis, University of Aberdeen (2015).